

CPT-based lateral displacement analysis using p - y method for offshore mono-piles in clays

Garam Kim, Donggyu Park, Doohyun Kyung and Junhwan Lee *

*Department of Civil and Environmental Engineering, Yonsei University,
134 Shinchon-dong, Seodaemun-gu, Seoul 120-749, Republic of Korea*

(Received August 27, 2013, Revised May 17, 2014, Accepted July 03, 2014)

Abstract. In this study, a CPT-based p - y analysis method was proposed for the displacement analysis of laterally loaded piles. Key consideration was the continuous soil profiling capability of CPT and cone resistance profiles that do not require artificial assumption or simplification for input parameter selection. The focus is on the application into offshore mono-piles embedded in clays. The correlations of p - y function components to the effective cone resistance were proposed, which can fully utilize CPT measurements. A case example was selected from the literature and used to validate the proposed method. Various parametric studies were performed to examine the effectiveness of the proposed method and investigate the effect of property profile and its depth resolution on the p - y analysis. It was found that the calculation could be largely misleading if wrongly interpreted sub-layer condition or inappropriate resolution of input soil profile was involved in the analyses. It was also found that there is a significant influence depth that dominates overall load response of pile. The soil profile and properties within this depth range affect most significantly calculated load responses, confirming that the soil profile within this depth range should be identified in more detail.

Keywords: p - y analysis; cone penetration tests; laterally loaded piles; offshore wind turbines; displacement analysis; undrained shear strength

1. Introduction

For offshore wind turbine structures, the installation of foundation costs around 21% of the total construction cost (IEA 2008), which is much higher than for inland wind turbines. Optimized foundation design and construction are particularly desired for offshore structures as great amount of construction cost can be saved. Among several, mono-piles are a common foundation type that is often adopted for offshore wind turbines for water depths shallower than around 30 to 40 m. The design of offshore mono-piles is similar to that of inland piles, while the lateral load response and lateral load carrying capacity are key design consideration as waves and winds are predominant load components.

The lateral load capacity of piles can be defined in two different aspects of the allowable load capacity (H_{all}) and the ultimate load capacity (H_u). H_u refers to failure of either soil or pile itself

*Corresponding author, Professor, E-mail: junlee@yonsei.ac.kr

while H_{all} is associated with the level of displacement that is tolerable for a given structure (Broms 1964, Duncan *et al.* 1994, Zhang *et al.* 2005). For the displacement analysis of laterally loaded piles for H_{all} , the beam-on-elastic foundation (BEF) approach based on the p - y analysis is often used (Matlock 1970, Reese *et al.* 1975, Duncan *et al.* 1994). The p - y analysis may be less rigorous than the continuum-based full numerical analysis as it is based on simplified soil springs and assumed load response curve. The p - y method has been however widely adopted in practice mainly due to the simplicity and reasonability of calculated results.

As for other foundation design and analysis, the adequacy of input parameters is crucially important for the successful implementation of the p - y analysis. When offshore environment is involved, the soil characterization using the conventional sampling- and testing-based approach is subjected to various experimental uncertainties with limited reliability of estimated soil parameters. For this reason, in-situ testing methods are preferred and regarded more effective for offshore cases (Titi *et al.* 2000, Tumay and Kurup 2001, Lee and Randolph 2011).

There have been several cases for the applications of in-situ test results into the p - y analysis (Briaud *et al.* 1985, Robertson *et al.* 1989, Gabr *et al.* 1994, Haldar and Babu 2009). Briaud *et al.* (1985) and Robertson *et al.* (1989) proposed the p - y analysis methods based on the pressure meter test (PMT) and dilatometer test (DMT) results, respectively. Gabr *et al.* (1994) also proposed a DMT-based p - y method using the hyperbolically defined load response curve. PMT and DMT were frequently adopted because the lateral loading mechanisms of the tests were similar to those of laterally loaded piles. Less attention has been given to the cone penetration test (CPT) mainly due to the different loading direction of the vertical cone penetration from the lateral pile loading process. However, it has been well recognized that the cone resistance is essentially governed by the horizontal effective stress rather than the vertical effective stress (Schnaid and Houlsby 1991). Moreover, it was recently found that the cone resistance is closely related to lateral pile load response as both are governed by the horizontal effective stress (Lee *et al.* 2010).

In the present study, a penetrometer-based p - y analysis method using CPT results is proposed for offshore piles embedded in clays. CPT is adopted to take advantage of the cost effectiveness and popularity in offshore soil investigation. The continuous profiling capability of CPT is an important consideration for the proposed method. The proposed CPT-based p - y analysis can take into account the depth variation of soil and layer profiles in detail by directly using CPT results. The effects of soil layering and property variation on the p - y analysis are examined in comparison to the conventional p - y analysis approach.

2. p - y analysis methods for laterally loaded piles in clays

The beam-on-elastic foundation (BEF) approach, often called as Winkler foundation, is a common approach in practice for the displacement analysis of laterally loaded piles. In this approach, as shown in Fig. 1, soils are assumed as a series of elastic springs with load responses defined by the p - y curves that are either linear or non-linear. Various p - y analysis methods have been proposed (Matlock 1970, Reese *et al.* 1975, Murchison and O'Neill 1984, Franke and Rollins 2013). The difference of the methods mainly come from the shape of p - y curve and definition of ultimate lateral resistance p_u .

For offshore piles embedded in clays, the method proposed by Matlock (1970) is often used and was adopted in various specifications (DNV 2004, API 2000). Matlock (1970) proposed a p - y curve shown in Fig. 2(a) applicable in soft clays. The function for the p - y curve of Matlock (1970) in Fig. 2(a) is given in a normalized form as follows

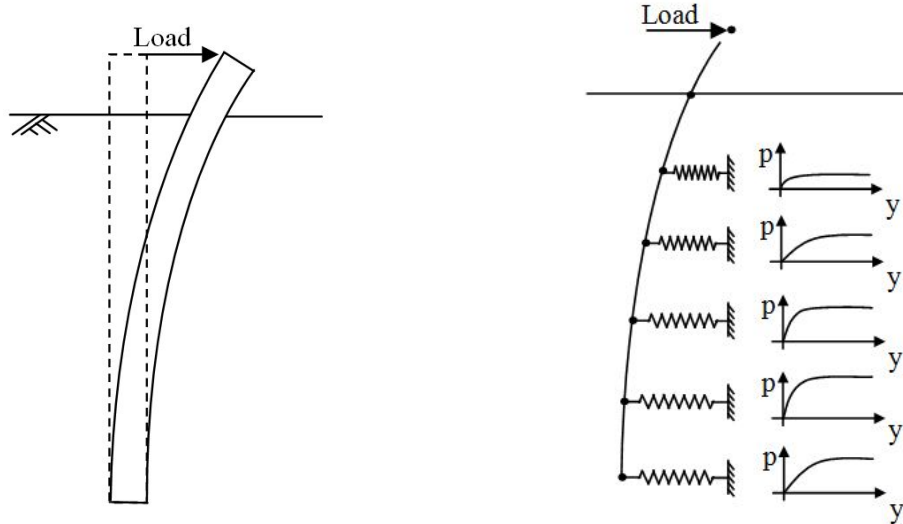


Fig. 1 p - y analysis model for laterally loaded piles

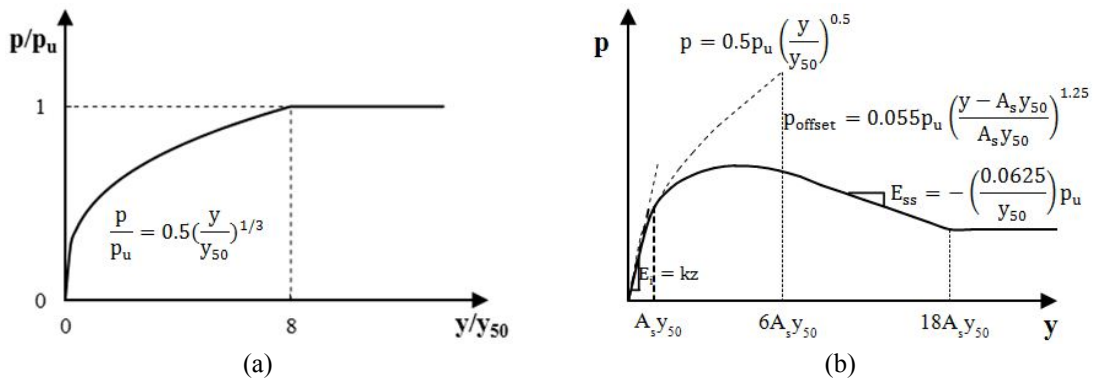


Fig. 2 p - y curve models for different clay conditions of: (a) soft clay (Matlock 1970); and (b) stiff clay (Reese *et al.* 1975).

$$\frac{p}{p_u} = 0.5 \cdot \left(\frac{y}{y_{50}} \right)^{1/3} \quad (1)$$

where p = lateral load per unit length; p_u = ultimate lateral soil resistance; y = induced lateral displacement; y_{50} = limit lateral displacement = $2.5 \cdot \varepsilon_{50} \cdot D$; ε_{50} = limit strain corresponding to 50% of failure stress in triaxial tests; and D = pile diameter. Beyond the lateral displacement of $8 \cdot y_{50}$, the value of p was set as a constant. In Eq. (1), p_u represents the ultimate resistance exerted by surrounding soils given as the following relationship

$$p_u = N_c \cdot s_u \cdot D \quad (2)$$

where s_u = undrained shear strength; N_c = bearing capacity factor; and D = pile diameter. N_c varies

from 3 to 9 depending on depth range given as follows

$$N_c = 3 + \frac{\gamma'z}{s_u} + \frac{Jz}{D} \quad (z < z_r) \quad (3)$$

$$N_c = 9 \quad (z \geq z_r) \quad (4)$$

where γ' = effective unit weight of soil; z = depth from ground surface; z_r = limit depth below ground surface; and J = empirical parameter that can be taken as 0.5 and 0.25 for soft and stiff clays, respectively. Eqs. (3)-(4) indicate that the value of N_c increases down to the limit depth z_r and then becomes constant equal to 9. According to Matlock (1970), the limit depth z_r can be estimated using the following relationship

$$z_r = \frac{6D}{\frac{\gamma'D}{s_u} + J} \quad (5)$$

For the cases in stiff over consolidated clays, Reese *et al.* (1975) proposed a p - y curve shown in Fig. 2(b) considering the stress softening behavior. The p - y curve of Reese *et al.* (1975) in Fig. 2(b) consists of 5 piecewise sections with functions given, respectively, as follows

$$p = (k \cdot z) \cdot y \quad (6)$$

$$p = 0.5p_u(y/y_{50})^{0.5} \quad (7)$$

$$p = 0.5p_u(y/y_{50})^{0.5} - 0.055p_u[(y - A_s y_{50})/(A_s y_{50})]^{2.5} \quad (8)$$

$$p = 0.5p_u(6A_s)^{0.5} - 0.411p_u - (0.0625/y_{50})p_u(y - 6A_s y_{50}) \quad (9)$$

$$p = 0.5p_u(6A_s)^{0.5} - 0.411p_u - 0.75p_u A_s \quad (10)$$

where k = subgrade reaction modulus; A_s = depth correction factor; and y_{50} = limit displacement = $\varepsilon_{50} \cdot D$. The depth correction factor A_s varies from 0.2 at the surface to 0.6 for depths greater than 3 times pile diameter ($3D$). p_u by Reese *et al.* (1975) is taken as the smaller one among the followings

$$p_u = 2\overline{s_u}D + \gamma'Dz + 2.83\overline{s_u}z \quad (11)$$

$$p_u = 11s_u D \quad (12)$$

where $\overline{s_u}$ = average undrained shear strength over the depth z ; and γ' = effective unit weight of clays.

For the displacement analysis using the p - y method in clays, as reviewed herein, key components are the magnitude of p_u and the function that defines the p - y curve, both of which are controlled by the effective stress and undrained shear strength. Although no particularly specific consideration has been addressed for the p - y analysis for offshore piles, the proper identification of

these parameters and their depth profiles is crucial, as it is often subjected to various uncertainties under offshore environment with larger variability than for inland cases.

3. Lateral displacement analysis using CPT results

3.1 Modified *p-y* function based on effective cone resistance

The soil reactions from the soil springs for the BEF approach vary with depth as a result of increasing stiffness and strength properties of the *p-y* curves. The undrained shear strength s_u is the governing soil variable for clays, which characterizes the main features of the *p-y* curve and the ultimate lateral soil resistance p_u . Various experimental methods have been proposed to estimate s_u (Ladd *et al.* 1977, Teh and Houlsby 1991, Stewart and Randolph 1994, Lunne *et al.* 2005). The typical examples of sampling-free, in-situ testing methods popular in practice include the field vane test (FVT) and cone penetration test (CPT). The cone penetration test can be particularly effective for offshore soils as the test is conducted by a single penetration process providing continuous and detailed depth profiles of seabed soil conditions.

The cone factor method is a common approach to estimate s_u using the CPT cone resistance given as the following relationship

$$s_u = \frac{q_t - \sigma_{v0}}{N_k} \quad (13)$$

where s_u = undrained shear strength; q_t = cone resistance; σ_{v0} = overburden total stress at cone tip level; and N_k = cone factor. As the cone factor method of Eq. (13) involves additional unknown parameter σ_{v0} , additional experimental procedure is required, which reduces the effectiveness of CPT application. As a recent development, the effective cone factor method was proposed, where s_u is given as a sole function of the cone resistance (Lee *et al.* 2010). The effective cone factor method is given by

$$s_u = \frac{q_t - u_0}{N_e} = \frac{q_e}{N_e} \quad (14)$$

where q_e = effective cone resistance = $q_t - u_0$; u_0 = hydrostatic pore pressure; and N_e = effective cone factor ≈ 16 . It is noted that no additional testing procedure is required for Eq. (14) as u_0 can be directly obtained from CPT results.

Introducing the effective cone factor into the ultimate lateral soil resistance p_u of Eq. (2), the following CPT-based p_u equation can be obtained

$$p_u = \frac{N_c}{N_e} \cdot D \cdot q_e \quad (15)$$

N_c and D in Eq. (15) are the bearing capacity factor and pile diameter, respectively. As N_c given by Eq. (3) varies with depth, the value of N_c/N_e also varies with depth. Below the limit depth z_r , however, N_c becomes constant as specified by Eq. (4). For depths greater than z_r , the values of N_c and N_e can be taken equal to 9 and 16, which produces the value of N_c/N_e equal to 0.5625. Using the p_u correlation of Eq. (15), the *p-y* function by Matlock (1970) can be modified in terms of the effective cone resistance q_e as follows

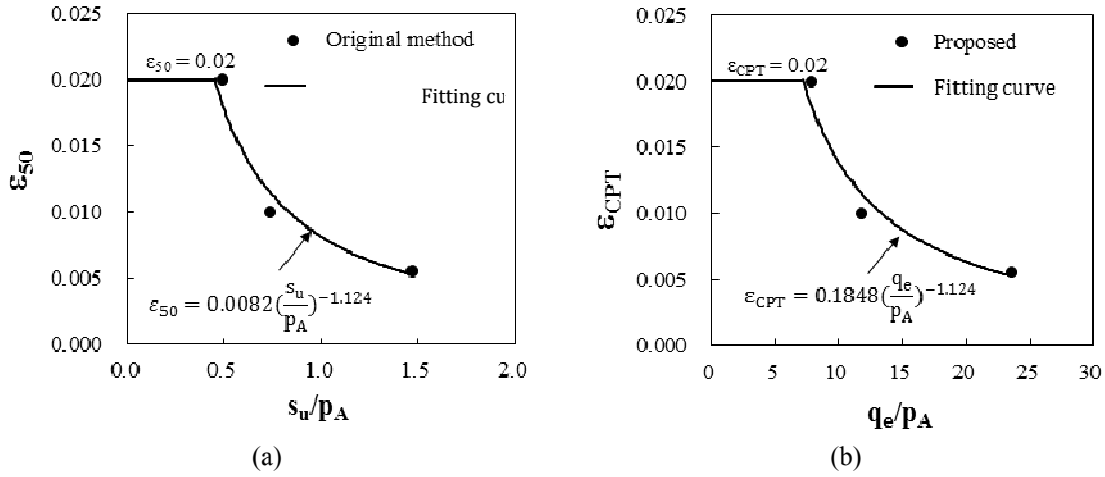


Fig. 3 Correlation of limit strain values for p - y method: (a) ε_{50} - s_u correlation; and (b) ε_{CPT} - s_u correlation

$$p = 0.5 \cdot \left(\frac{N_c}{N_e} \right) \cdot q_e \cdot D \cdot \left(\frac{y}{y_{50}} \right)^{1/3} \tag{16}$$

Note that, as Eq. (16) does not involve the overburden stress σ_{v0} , the continuous cone resistance profiles from CPT can be fully utilized into the analysis.

According to Matlock (1970), the limit displacement y_{50} can be evaluated by using the limit strain value ε_{50} based on the stress-strain curve of the clay at the site. As the original method specifies the discretized values of ε_{50} for a given range of s_u as indicated in Fig. 3(a), a fitting curve was obtained and included in Fig. 3(a) to describe the ε_{50} - s_u correlation. Following the effective cone resistance of Eq. (14), the ε_{50} - s_u correlation in Fig. 3(a) can be further modified in terms of the effective cone resistance as plotted in Fig. 3(b). ε_{CPT} in Fig. 3(b) can be directly estimated from CPT cone resistances. Note that all correlations given in Fig. 3 were fit to be compatible to the existing results adopted in current practice. Skempton (1951) and Matlock (1970) suggested the values of ε_{50} in the range from 0.02 to 0.005 for most clayey soils. The maximum value of ε_{50} and ε_{CPT} equal to 0.02 given in Fig. 3 was also set to maintain the consistency with the value specified in the original method. The ε_{CPT} - q_e correlation given in Fig. 3(b) is

$$\varepsilon_{CPT} = 0.185 \cdot \left(\frac{q_e}{p_A} \right)^{-1.124} \leq 0.02 \tag{17}$$

where q_e = effective cone resistance; p_A = reference stress = 100 kPa. Using Eqs. (16)-(17), the modified CPT-based p - y function is then obtained as follows

$$p = 0.368 \cdot \left(\frac{N_c}{N_e} \right) \cdot q_e \cdot \left(\frac{yD^2}{\varepsilon_{CPT}} \right)^{1/3} \tag{18}$$

The value of N_c/N_e varies down to the depth of z_r , below which it is equal to 0.5625. As the

proposed p - y function of Eq. (18) utilizes the continuous CPT profile, any changes in depth profile of soil characteristics can be readily considered into the analysis without a need of assumed simplification or idealization of in-situ soil profiles.

3.2 Load transfer analysis and calculation

The load-transfer analysis is the main calculation step in the BEF approach using the p - y curve for the displacement analysis of laterally loaded piles. It simulates the load responses of assumed pile segments and soil springs upon lateral loading. The schematic illustration of load-transfer mechanism is shown in Fig. 4. A series of pile segments with the length of h are connected at nodes where the shear stress (V), axial stress (Q) and bending moment (M) are transferred. At each node, the bending stiffness is introduced in terms of the elastic modulus (E) and the second moment of inertia (I).

The governing differential equation for the equilibrium condition of a pile segment shown in Fig. 4(b) is given by

$$EI \frac{d^4 y}{dz^4} + Q \frac{d^2 y}{dz^2} - p + W = 0 \tag{19}$$

where EI = flexural rigidity of pile; Q = axial load; p = soil reaction per unit length; and W = distributed load along pile. Applying the finite difference scheme, the governing differential equation of Eq. (19) can be rewritten as the following discretized formulation

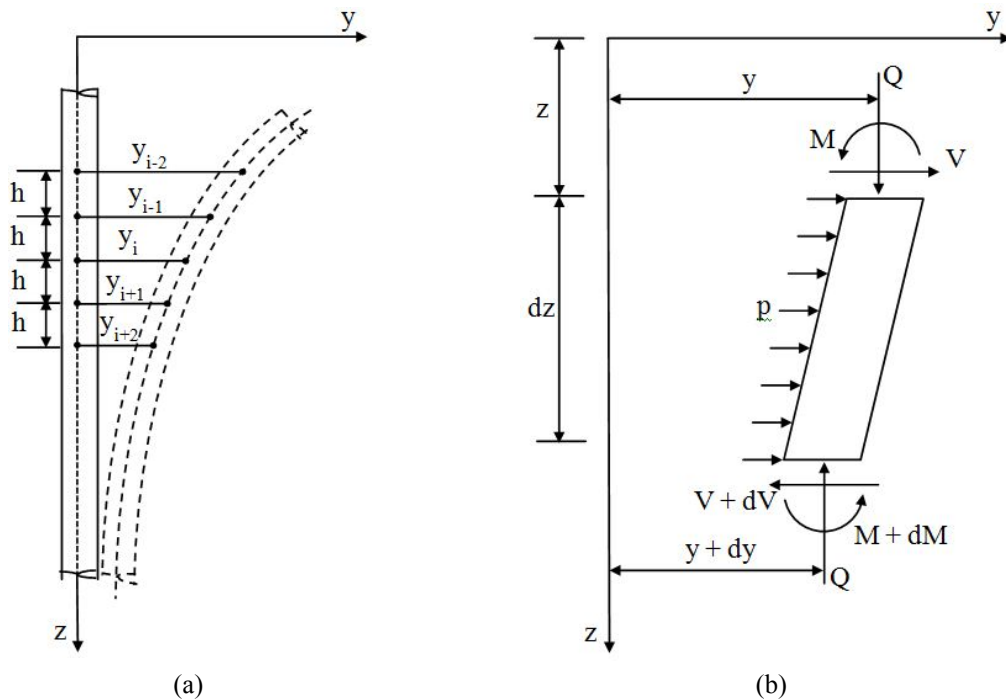


Fig. 4 Configuration of laterally loaded piles: (a) lateral deflection of pile segments and (b) forces acting on elementary pile segment

$$a_i \cdot y_{i-2} + b_i \cdot y_{i-1} + c_i \cdot y_i + d_i \cdot y_{i+1} + e_i \cdot y_{i+2} = f_i \quad (20)$$

where a , b , c , d , e , and f are model coefficients. The subscript i represents the node number of discretized pile segments. Each model coefficient in Eq. (20) is given by

$$a_i = R_{i-1} \quad (21)$$

$$b_i = -2R_{i-1} - 2R_{i+1} + Qh^2 \quad (22)$$

$$c_i = R_{i-1} + 4R_i + R_{i+1} - 2Qh^2 + E_{pyi}h^4 \quad (23)$$

$$d_i = -2R_i - 2R_{i+1} + Qh^2 \quad (24)$$

$$e_i = R_{i+1} \quad (25)$$

$$f_i = -Wh^4 \quad (26)$$

where R_i = flexural rigidity at node $i = (EI)_i$ and E_{pyi} = secant modulus of soil springs at node i from the proposed p - y curve of Eq. (18). If lateral load imposed on pile head is the only external load, Q and W are set equal to zero.

The model coefficients of Eqs. (21)-(26) can be determined from the system equations established for the assigned nodes between pile segments and two additional imaginary nodes assigned at the top and bottom ends of pile. If the pile is divided into n segments, $n + 5$ nodes are generated and thus $n + 5$ equations are established. If boundary conditions are given at the top and bottom of pile, the set of algebraic equations for the assigned nodes can be solved.

At the bottom of pile, the boundary condition is set as zero-bending moment and zero-shear given as follows

$$y_{-1} - 2y_0 + y_1 = 0 \quad (27)$$

$$\frac{R_0}{2h^3}(y_{-2} - 2y_{-1} + 2y_1 - y_2) + \frac{Q}{2h}(y_{-1} - y_1) = V_0 \quad (28)$$

where, y_{-2} , y_{-1} , y_0 , y_1 , y_2 = lateral deflections defined at the bottom segment and imaginary nodes of pile shown in Fig. 5(a); R_0 = flexural rigidity at the bottom node of pile = $(EI)_0$, h = segment length, Q = axial load, and V_0 = shear force at the bottom node of pile. Note that the assumption of zero-bending moment and zero-shear is applicable for long flexible piles and short rigid piles that show rotation behavior upon lateral load as assumed in most cases. However, if a pile is short rigid and yet fixed at base, the bending moment would be generated at pile base and the assumption of zero-bending moment at pile base would be not be valid (Reese *et al.* 1970).

For the top boundary condition for free head illustrated in Fig. 5(b), the following equations for moment and force equilibriums are imposed

$$\frac{R_t}{h^2}(y_{t-1} - 2y_t + y_{t+1}) = M_t \quad (29)$$

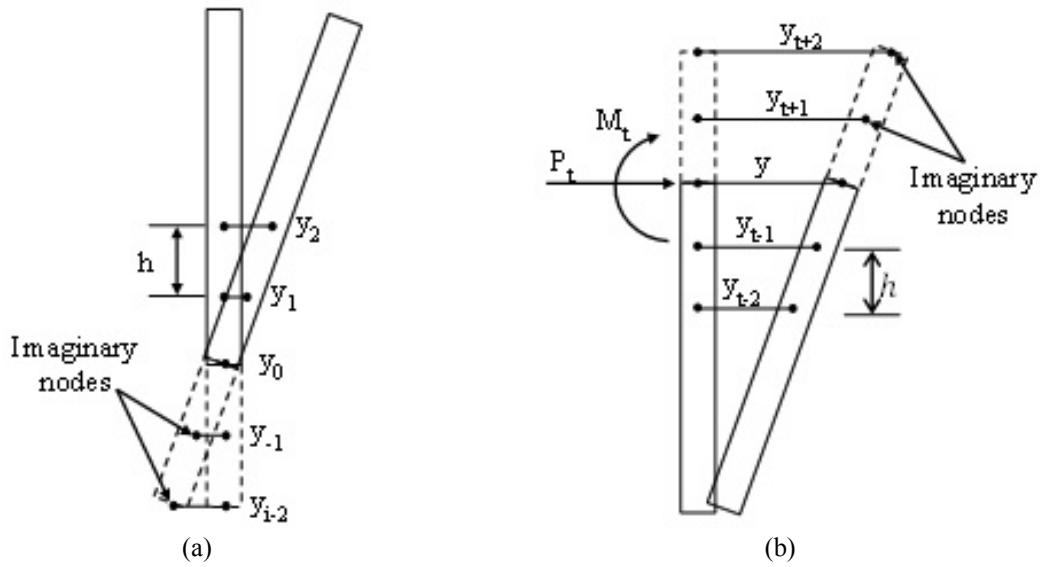


Fig. 5 Node configuration for boundary conditions: (a) bottom boundary of pile; and (b) top boundary of pile

$$\frac{R_t}{2h^3}(y_{t-2} - 2y_{t-1} + 2y_{t+1} - y_{t+2}) + \frac{Q}{2h}(y_{t-1} - y_{t+1}) = P_t \tag{30}$$

where, M_t and P_t = bending moment and shear force at the top node of pile, y_{t-2} , y_{t-1} , y_t , y_{t+1} , y_{t+2} = lateral deflections at the top segment and imaginary nodes of pile shown in Fig. 5(b), R_t = flexural rigidity at the top node of pile = $(EI)_t$.

In a matrix form, the governing equation of Eq. (20) can be given as follows

$$[A] \cdot (y) = (f) \tag{31}$$

where $[A]$ = stiffness matrix; (y) = lateral displacement vector matrix; and (f) = load vector matrix. The stiffness matrix $[A]$ contains the system equations of the model parameters and boundary conditions given by Eqs. (21)-(30). The lateral displacement vector of pile can be obtained taking $[A]^{-1}$ for each side.

3.3 Calculation algorithm

The load transfer mechanism and the proposed CPT-based p - y analysis method described previously were programmed using the commercial programming software MATLAB. Fig. 6 shows the schematic flow and steps of the developed program for the calculation algorithm using the proposed method. The developed program is composed of three main parts. The first part includes the input process of required soil and pile parameters, division of pile segments, node assignment, and construction of the p - y curve. As the cone resistance and its depth profile are used as input soil parameters, CPT results obtained from field are directly introduced into the program. ε_{CPT} and p_u are then calculated to construct the p - y curves at each node, which is incorporated into the main calculation step of the load-transfer analysis. The second part consists of assembling the stiffness

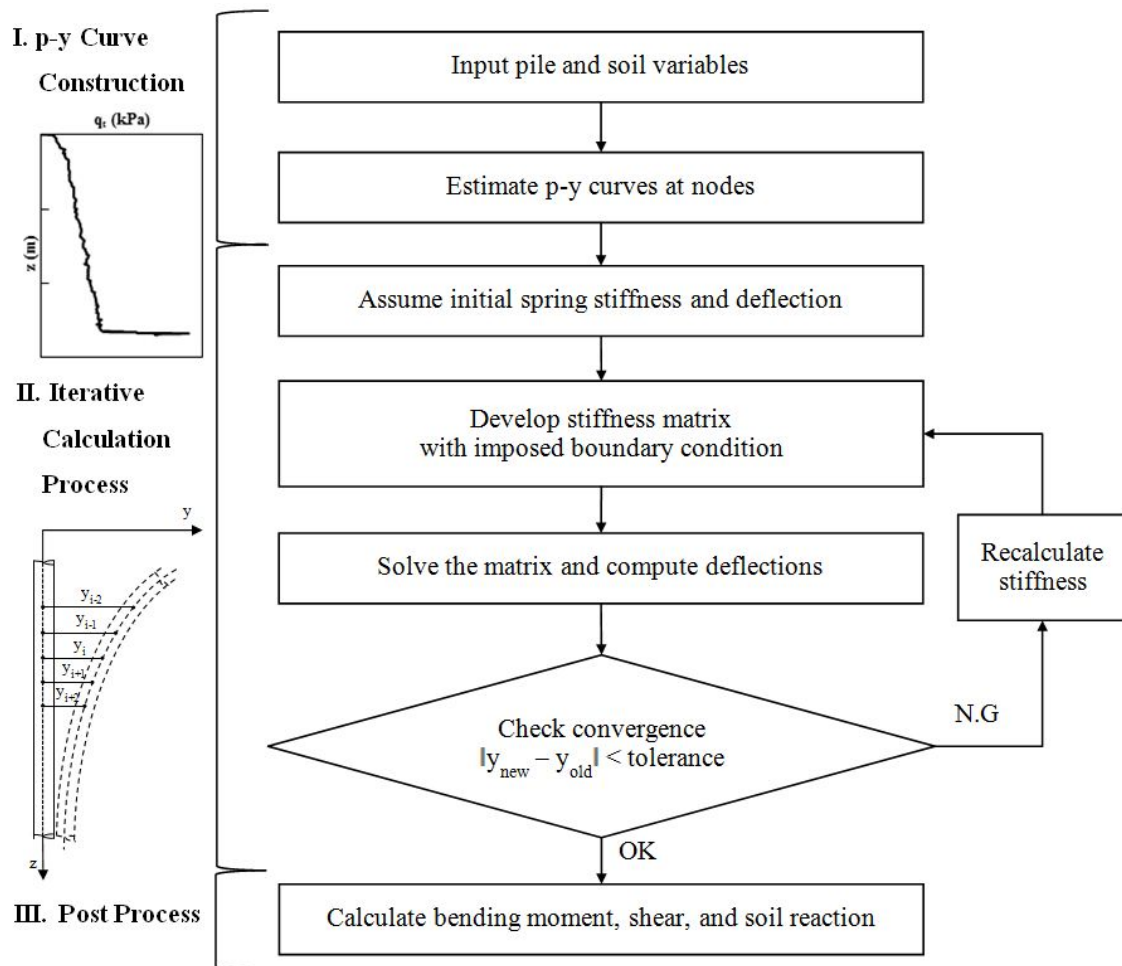


Fig. 6 Calculation flow and algorithm

matrix for the system equations and solving the matrix equation by iteration. The five-diagonal banded matrix is created with the coefficients given by Eqs. (21)-(26) at nodes. The set of algebraic equations are then solved for lateral pile deflections using the inverse matrix and imposed boundary conditions at the top and bottom of pile. The third, final step is to calculate the bending moments, shear forces, and soil reactions along pile from calculated lateral deflections.

4. Comparison and validation

To check the validity of the proposed CPT-based p - y analysis method, a case example was selected from the literature and used to compare measured and calculated lateral load responses. The selected example is a field lateral pile load test by Rollins *et al.* (1998), conducted at Salt Lake City, Utah in USA. Various in-situ and laboratory tests were conducted to characterize the soils at

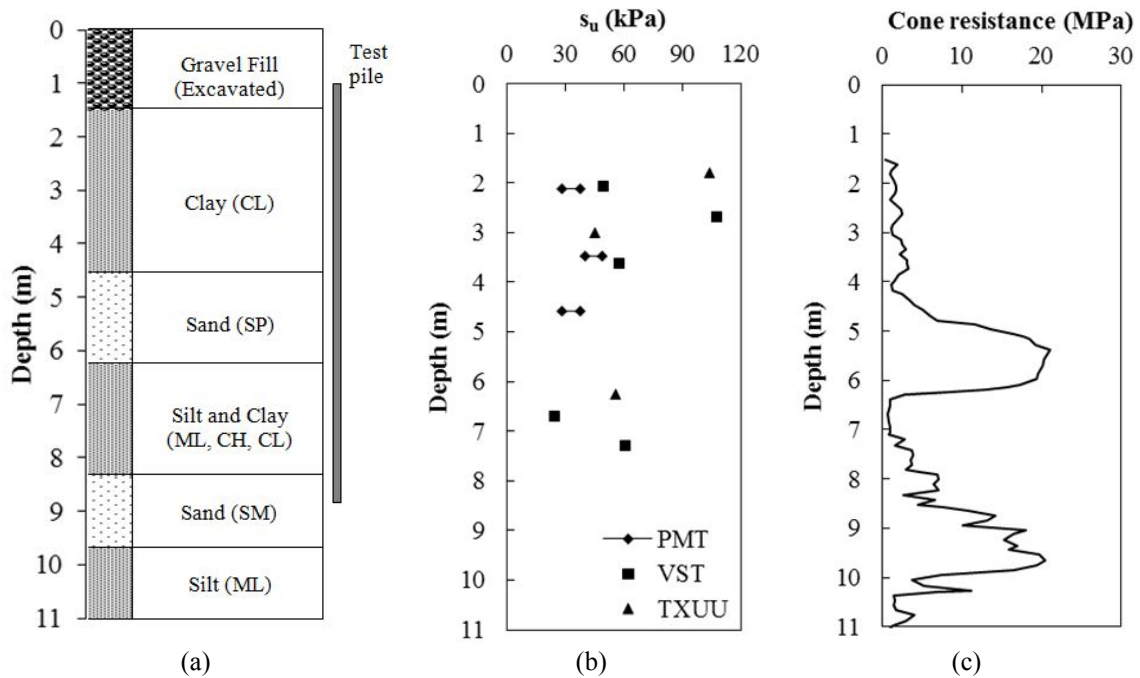


Fig. 7 Soil parameter at test site: (a) soil profile; (b) undrained shear strength profile; and (c) CPT profile

the test site, including the standard penetration test (SPT), cone penetrometer test (CPT), dilatometer test (DMT), pressuremeter test (PMT), field vane test (FVT), and other fundamental laboratory tests.

The soil profile at the test site showed a composite soil layering condition with clay, silt, and some sand layers. Fig. 7(a) shows the depth profiles of soil type at the test site. There was a gravel fill layer near surface, which was excavated before the test pile installation. Low-plasticity silts and clays existed within the depths of 1.7 m to 4.5 m. The depth profiles of undrained shear strength s_u and CPT cone resistance are given in Figs. 7(b)-(c), respectively. It is seen that the values of s_u were typically in the range between 25 and 60 kPa while some exceptionally higher values around 100 kPa were observed near surface due to the over consolidated stress condition. The cone resistances were lower than 3 MPa for the clay layer down to the depth of 4 m and higher cone resistances were observed for the sand layer between the depths of 4.5 to 6.2 m. The test pile was made of close-ended steel pipe with an inside diameter equal to 314.5 mm. The embedded pile depth was 7.9 m with the vertical load eccentricity above the ground of 0.4 m.

The p - y analysis was performed using both results of s_u and q_t given in Figs. 7(b)-(c), respectively. For the CPT-based p - y analysis, the proposed method was adopted while the original Matlock's method was used for the s_u -based p - y analysis with the well-known commercial program LPILE (Reese *et al.* 2004). For the input s_u profiles for LPILE, two differently assumed profiles were prepared and adopted into the p - y analysis. One is a simplified profile using a single average value of s_u for a given layer and the other is a detailed profile reflecting most significant variation of s_u within the layers. These two assumed profiles are shown in Fig. 8. For the proposed method, the CPT profile given in Fig. 7(c) was adopted. For the calculation within the sand layers, the API method (API 2000) was used.

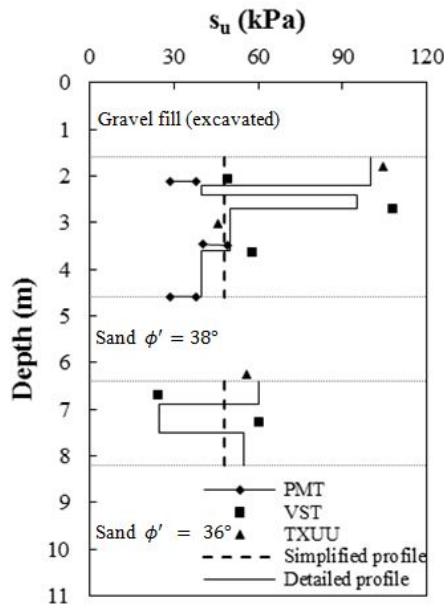


Fig. 8 Undrained shear strength profiles

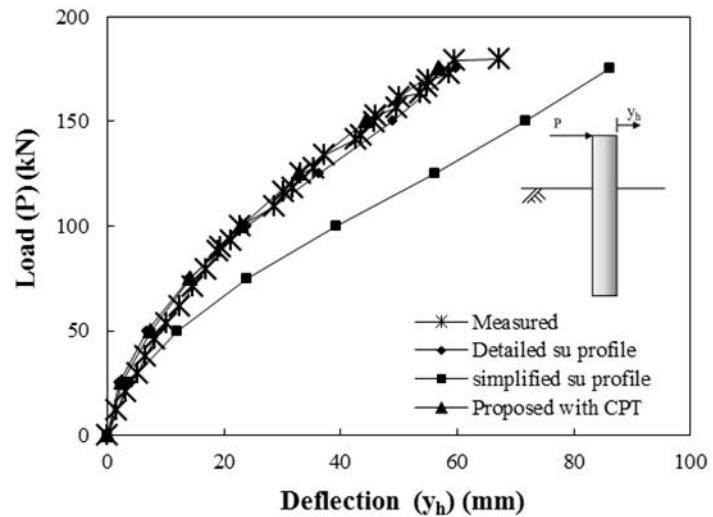


Fig. 9 Measured and predicted pile head deflections

Fig. 9 shows measured and calculated lateral load responses. It is seen that the calculated results using the proposed CPT-based method and detailed s_u -profile are both in similarly close agreement with the measured curve. The simplified s_u -profile on the other hand produced underestimated lateral load response. While the results in Fig. 9 validates the proposed CPT-based method, it is also indicated that the resolution of depth profile for the input parameters plays an important role in the p - y analysis and affect significantly calculated load responses.

5. Effect of property profile and soil layer condition

5.1 Effect of profile resolution

The main advantage of the proposed CPT-based p - y analysis is that detailed soil profiles, often with complexity, can be readily considered in the analysis without additional sampling and testing procedure. It is distinguished from the conventional way that utilizes individual property values with a certain depth interval. The effectiveness of the proposed method would differ depending on the soil profile and layering conditions. In order to investigate the effect of property profile and its depth resolution on the p - y analysis, a series of clay soil deposits were assumed and parametric study was performed. The assumed soil profiles were defined using the following s_u profile relationship

$$s_u = \alpha \cdot z \quad (32)$$

where s_u = undrained shear strength; α = strength increase factor; and z = depth. While the range of α values for *NC* clays is typically between 1 and 2, the α values equal to 0.5, 1, 2, and 3 were considered in the analyses to cover full range of possible clay conditions. The assumed soil

conditions are shown in Fig. 10(a).

The assumed s_u profiles shown in Fig. 10(a) were divided into several sub-layers and average s_u values were assigned for each sub-layer as input values for the p - y analysis. Fig. 10(b) shows examples of the considered sub-layer conditions adopted in the p - y analysis. Note that, for all the cases shown in Fig. 10(b), the values of average s_u along the pile embedded depth are the same. In order to consider the effect of pile rigidity, different EI values for the pile, equal to 0.5×10^6 , 1.0×10^6 and 1.5×10^6 kN·m, were considered. The total pile length was 35 m with the pile embedded depth of 30 m.

Fig. 11 shows lateral deflections (y) at pile head [Fig. 11(a)] and the maximum bending moments (M_{max}) [Fig. 11(b)] with the number of sub-layer for different s_u profile conditions. The lateral load and EI of the pile in Fig. 11 was 100 kN and 1.0×10^6 kN·m, respectively. In Fig. 11, the values of y and M_{max} were normalized with those obtained for the original continuous s_u profile (i.e., y_0 and $M_{max,0}$). The single sub-layer case produced the values of y and M_{max} underestimated by around 40% and 72% compared to those for the continuous s_u profile. As the number of sub-layer increases, the difference became smaller. For the cases with more than 5 sub-layers, calculated results showed the degrees of match higher than 90% to y_0 and $M_{max,0}$. Similar result were obtained for the other pile cases with $EI = 0.5 \times 10^6$ and 1.5×10^6 kN·m. These confirm that the calculated results of the p - y analysis are significantly affected by assumed sub-layer condition and resolution of input soil profile, justifying the effectiveness of the proposed CPT-based method.

5.2 Significant influence layer depth

The depths or thicknesses of sub-layers affect the lateral pile load responses as the p - y behavior changes with depth. If there is a depth range within which the soil condition dominates the overall

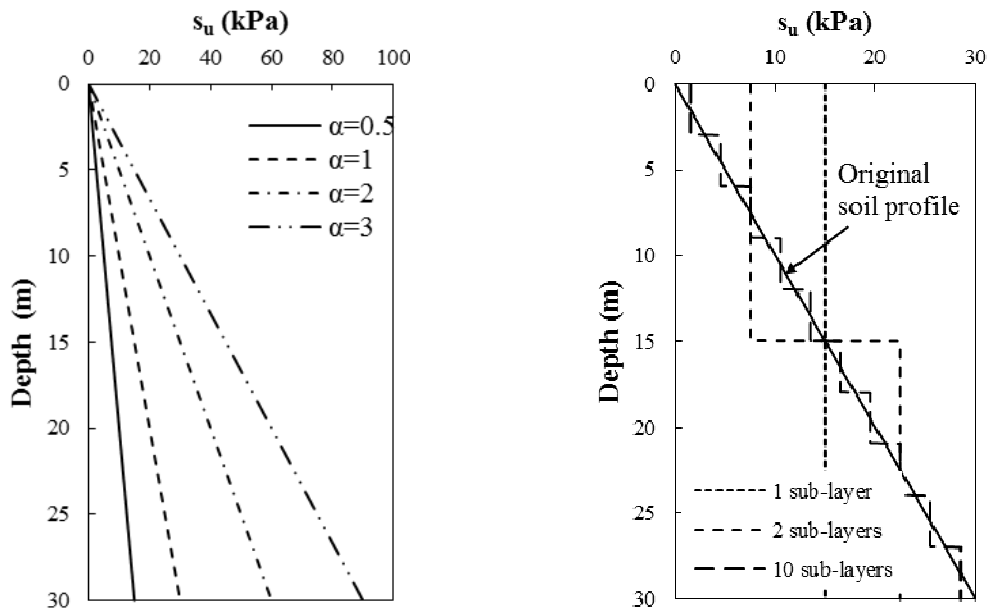


Fig. 10 Soil profiles for parameter study: (a) assumed s_u -profiles; and (b) assumed sub-layer conditions

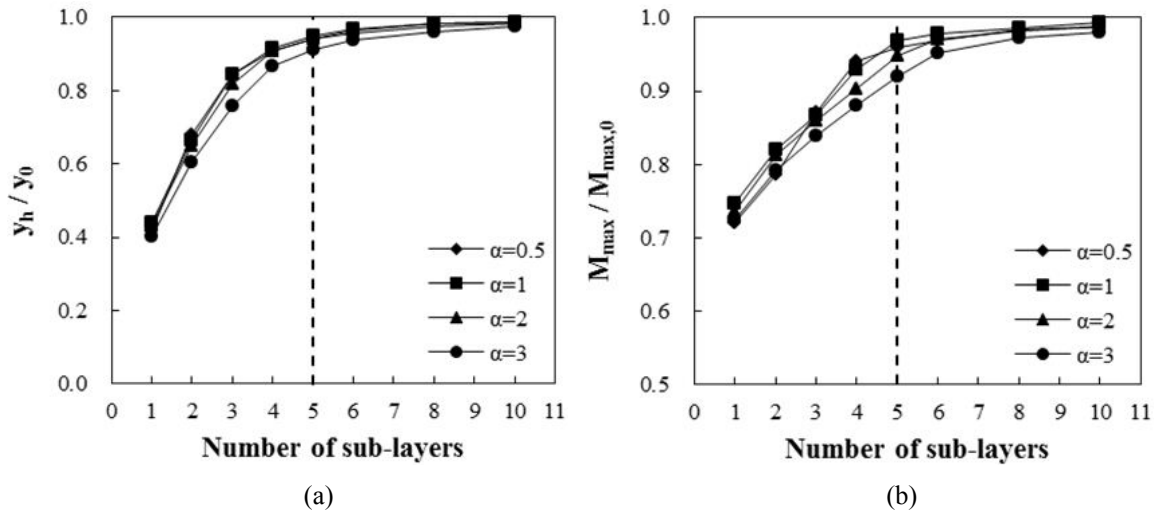


Fig. 11 Normalized deflections and bending moments: (a) normalized head deflections; and (b) normalized maximum bending moments

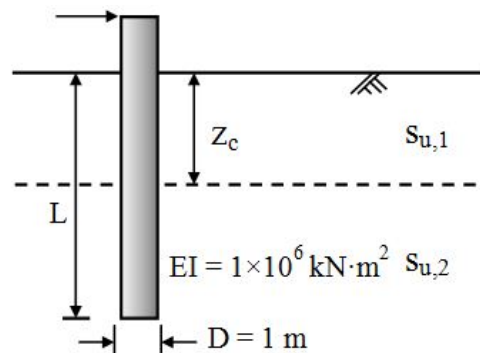


Fig. 12 Assumed soil sub-layer and pile conditions for parameter study

lateral load response of the pile, input soil variables within this significant influence depth range should be identified in more detail. To analyze the significant influence depth range, additional parametric study was performed assuming different soil layer conditions. The assumed soil conditions consisted of two sub-layers with different layer thicknesses as illustrated in Fig. 12. The undrained shear strengths (s_u) for the upper and lower sub-layers were designated as $s_{u,1}$ and $s_{u,2}$, respectively. z_c in Fig. 12 represents the thickness of the upper sub-layer.

For the parametric study, two groups of soil conditions were considered. $s_{u,1}$ of the first group is greater than $s_{u,2}$ and the other group represents the opposite condition. For each group, different values of $s_{u,1}$ and $s_{u,2}$ were considered. Two different pile lengths of 15 and 30 m were considered to check the results for both short (rigid) and long (flexible) pile conditions. Short and long piles in this study were classified based on the pile characteristic length (βL) proposed by Broms (1964). Short piles correspond to βL smaller than 2.3. The values of pile characteristic length parameter [$\beta = (E_s/E_p I_p)^{1/4}$] were calculated for each given soil and pile conditions. The values of the characteristic pile length (βL) for the 15-m pile were between 1.8 and 2.2 indicating short piles.

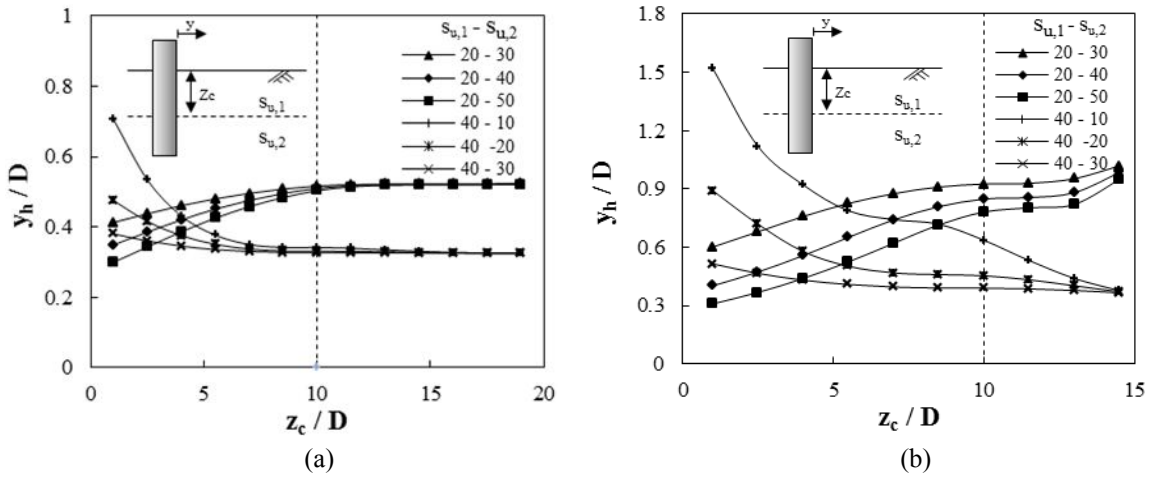


Fig. 13 Calculated head deflection for different sub-layer thickness condition for: (a) long flexible; and (b) short rigid and piles

The 30-m pile was classified into a long pile as βL ranged from 3.7 to 4.5.

Figs. 13(a)-(b) show calculated pile head deflections (y) from the p - y analysis as a function of z_c for the long and short pile cases, respectively. Both z_c and y in Fig. 13 were normalized with the pile diameter (D) of 1 m. The results obtained for different s_u conditions were all included in the figure. As shown in Fig. 13(a) for the long pile case, no significant changes in the calculated pile deflections are observed for z_c greater than $10D$. This means that input soil profile down to the depth of $10D$ dominates calculated lateral load responses and the effect of soil profile below $10D$ is minor. However, for the short pile case with $L = 15D$ in Fig. 13(b), no converged values of z_c are observed, indicating the soil profile throughout the entire pile embedded depth contributes the overall load response. This represents that the soil profile identification becomes more important for short pile cases and the proposed method with detailed soil profiling would be more beneficial.

6. Conclusions

In this study, a CPT-based p - y analysis method was proposed for the displacement analysis of laterally loaded piles. Key consideration was the continuous soil profiling capability of CPT and cone resistance profiles that do not require artificial assumption or simplification for input parameter selection. The proposed method is focused on the application into mono-piles embedded in offshore clayey soils where the soil characterization is limited. The correlations of p - y function components to the effective cone resistance were proposed, which can fully utilize CPT measurements.

The proposed CPT-based p - y model and the load transfer calculation procedure were programmed and used to obtain load responses of laterally loaded piles. A case example was selected from the literature and used to compare measured and calculated results. Close match was observed from the results measured and using the proposed method. It was indicated that the resolution of depth profile for input parameters in the p - y analysis is important and affect significantly calculated load responses.

Various parametric studies were performed to examine the effectiveness of the proposed CPT-based method and investigate the effect of property profile and its depth resolution on the p - y analysis. A series of assumed clay soil deposits were prepared and introduced into the calculation and comparison of load responses of laterally loaded piles. It was found that the calculation could be largely misleading if wrongly interpreted sub-layer condition or inappropriate resolution of input soil profile was involved in the analysis. From the analysis of the significant influence depth range, it was found that there is a depth range where the soil profile and properties affect the calculated load responses, consequently dominating the overall load response. It was also found that the soil profile identification becomes more important for short piles indicating that the proposed method with detailed soil profiling would be more beneficial.

Acknowledgments

This research was supported by Basic Science Research Program through the National Research Foundation of Korea(NRF) funded by the Korea government (MSIP) (No. 2011-0030040) and the Ministry of Education(No.2013R1A1A2058863).

References

- API (2000), *Recommended Practice for Planning, Designing and Construction Fixed Offshore Platforms - Working Stress Design*, American Petroleum Institute, API Recommended Practice 2A-WSD (RP2A-WSD), (21st Edition), Dallas, TX, USA.
- Broms, B.B. (1964), "Lateral resistance of piles in cohesive soils", *J. Soil Mech. Found. Div. - ASCE*, **90**(2), 27-63.
- Briaud, J.L., Tucker, L., Lytton, R.L. and Coyle, H.M. (1985), "Behavior of piles and pile groups in cohesionless soils", Final Report, Report No. FHWA/RD-83/038, NTIS PB86-152089/AS.
- DNV (2004), Det Norske Veritas, *Design of Offshore Wind Turbine Structures*, Offshore Standard, Norway.
- Duncan, J., Evans, L. Jr. and Ooi, P. (1994), "Lateral load analysis of single piles and drilled shafts", *J. Geotech. Eng., ASCE*, **120**(6), 1018-1033.
- Franke, K. and Rollins, K. (2013), "Simplified hybrid p - y spring model for liquefied soils", *J. Geotech. Geoenviron. Eng., ASCE*, **139**(4), 564-576.
- Gabr, M., Lunne, T. and Powell, J. (1994), " P - y analysis of laterally loaded piles in clay using DMT", *J. Geotech. Eng., ASCE*, **120**(5), 816-837.
- Haldar, S. and Babu, G.S. (2009), "Design of laterally loaded piles in clays based on cone penetration test data: A reliability-based approach", *Géotechnique*, **59**(7), 593-607.
- IEA (2008), *World Energy Outlook 2008*, International Energy Agency, Paris, France.
- Ladd, C.C., Foot, R., Ishihara, K., Schlosser, F. and Poulos, H.G. (1977), "Stress-deformation and strength characteristics, state of the art report", *Proceedings of the 9th ISMFE*, Tokyo, **Vol. 4**, pp. 421-494.
- Lee, J., Kim, M. and Kyung, D. (2010), "Estimation of lateral load capacity of rigid short piles in sands using CPT results", *J. Geotech. Geoenviron. Eng., ASCE*, **136**(1), 48-56.
- Lee, J. and Randolph, M. (2011), "Penetrometer-based assessment of spudcan penetration resistance", *J. Geotech. Geoenviron. Eng., ASCE*, **137**(6), 587-596.
- Lee, J., Seo K., Kang, B., Cho, S. and Kim, C. (2010), "Application of effective cone factor for strength characterization of saturated clays", *Proceedings of GeoFlorida 2010 (Advances in analysis, modeling and design)*, West Palm Beach, FL, USA, February.
- Lunne, T., Randolph, M.F., Chung, S.F., Anderson, K.H. and Sjursen, M.A. (2005), "Comparison of cone T-bar factors in two onshore and one offshore clay sediments", *Proceedings of the 1st International*

- Symposium on Frontiers in Offshore Geotechnics*, Perth, WA, USA, September, pp. 981-989.
- Matlock, H. (1970), "Correlation for design of laterally loaded piles in soft clay", *The 2nd Annual Offshore Technology Conference*, Houston, TX, USA, April, pp. 577-607.
- Murchison, J.M. and O'Neill, M.W. (1984), "Evaluation of p - y relationships in cohesionless soils", *Anal. Des. Pile Found.*, ASCE, 174-191.
- Reese, L.C., Cox, W.R. and Koop, F.D. (1975), "Field testing and analysis of laterally loaded piles in stiff clay", *Proceedings of Offshore Technology Conference*, Houston, TX, USA, May, pp. 671-690.
- Reese, L.C., Wang, S.T., Isenhower, W.M., Arrellaga, J.A. and Hendrix, J. (2004), *Computer Program: LPILE Version 5 Technical Manual*, Ensoft Inc., Austin, TX, USA.
- Robertson, P.K., Davis, M.P. and Campanella, R.G. (1989), "Design of laterally loaded driven piles using the flat dilatometer", *Geotech. Test. J.*, **12**(1), 30-38.
- Rollins, K., Peterson, K. and Weaver, T. (1998), "Lateral load behavior of full-scale pile group in clay", *J. Geotech. Geoenviron. Eng.*, ASCE, **124**(6), 468-478.
- Rollins, K.M., Johnson, S.R., Petersen, K.T. and Weaver, T.J. (2003), "Static and dynamic lateral load behavior of pile groups based on full-scale testing", *Proceedings of the 13th International Offshore and Polar Engineering Conference*, Honolulu, Hawaii, USA, May.
- Schnaid, F. and Houlsby, G.T. (1991), "An assessment of chamber size effects in the calibration of in situ tests in sand", *Géotechnique*, **41**(3), 437-445.
- Skempton, A.W. (1951), "The bearing capacity of clays", *Proceedings, Building Research Congress, Division 1*, London, England, pp.180-189.
- Stewart, D. and Randolph, M. (1994), "T-bar penetration testing in soft clay", *J. Geotech. Eng.*, ASCE, **120**(12), 2230-2235.
- Teh, C.I. and Houlsby, G.T. (1991), "An analytical study of the cone penetration test in clay", *Géotechnique*, **41**(1), 17-34.
- Titi, H.H., Mohammad, L.N. and Tumay, M.T. (2000), "Miniature cone penetration tests in soft and stiff clays", *Geotech. Test. J.*, ASTM, **23**(4), 432-443.
- Tumay, M.T. and Kurup, P.U. (2001), "Development of a continuous intrusion miniature cone penetration test system for subsurface explorations", *Soil. Found.*, **41**(6), 129-138.
- Zhang, L., Silva, F. and Grismala, R. (2005), "Ultimate lateral resistance to piles in cohesionless soils", *J. Geotech. Geoenviron. Eng.*, ASCE, **131**(1), 78-83.